

THE UNIVERSITY OF MICHIGAN

COLLEGE OF ENGINEERING

Department of Engineering Mechanics

Department of Mechanical Engineering

Tire and Suspension Systems Research Group

Technical Report No. 18

AN ANALOG FOR THE STATIC LOADING  
OF A PNEUMATIC TIRE

S. K. Clark

Project Director: S. K. Clark

ORA Project 02957

administered through:

OFFICE OF RESEARCH ADMINISTRATION

ANN ARBOR

January 1964

Revised March 1964

ENGM

UNR1243

The Tire and Suspension Systems Research Group  
at The University of Michigan is sponsored by:

FIRESTONE TIRE AND RUBBER COMPANY

GENERAL TIRE AND RUBBER COMPANY

B. F. GOODRICH TIRE COMPANY

GOODYEAR TIRE AND RUBBER COMPANY

UNITED STATES RUBBER COMPANY

## TABLE OF CONTENTS

	Page
LIST OF FIGURES	vii
NOMENCLATURE	ix
I. FOREWORD	1
II. SUMMARY	2
III. EQUATIONS OF EQUILIBRIUM	3
IV. CONTACT PATCH LENGTH	10
V. COMPARISON OF CALCULATION AND EXPERIMENT	14
VI. STRESSES IN THE RUNNING BAND, OR TREAD, REGION	20
VII. REFERENCES .	25
VIII. DISTRIBUTION LIST	26

## LIST OF FIGURES

Figure	Page
1. Circular shell in a state of plane stress, or two-dimensional loading.	3
2. Deformed and undeformed states of thin, circular shell.	3
3. Actual contact patch length vs. geometric intersection length.	8
4. Geometry of intersection of a circle and a plane.	11
5. Plot of contact patch length vs. vertical tire deflection.	15
6. Photograph of tire used to obtain data appearing in Fig. 5.	16
7. Plot of footprint-length parameter vs. vertical-deflection parameter.	19
8. Critical pressure necessary to maintain tension in the running band.	23

## NOMENCLATURE

### English Letters

a	undeformed radius of cylindrical shell
b	width of cylindrical shell
c	distributed damping constant of shell's elastic foundation
E	Young's modulus
g	gravitational constant
h	shell thickness
H	tire deflection
k	elastic modulus of shell internal foundation
P	a material point
p	pressure
r	deformed radius of shell at point P
t	time
w	deflection

### Greek Letters

$\alpha$	dimensionless quantity
$\epsilon$	strain
$\theta$	original angle in undeformed state
$\phi$	final angle in deformed state
$\zeta$	dimensionless deflection
$\rho$	density

## NOMENCLATURE (Concluded)

$\psi$  angular deformation

$\tau$  dimensionless time

$\omega$  angular velocity

### Subscripts

$\phi$  circumferential

0 pertaining to geometric intersection of plane and wheel

## I. FOREWORD

This report discusses the first of a series of pneumatic tire problems which can be well represented by an analog to a pneumatic tire, this analog being composed of an elastic body which exhibits characteristics such that:

1. Motion in the plane of the wheel is approximately represented by the same set of equations which defines the deformation of a circular cylindrical shell.
2. Motion transverse to the plane of the wheel is approximately represented by the same set of equations which defines the deformation of a beam on an elastic foundation, as has been pointed out by Saito<sup>1</sup> and, before him, Thorsen.<sup>2</sup>

It is believed that this analog will open immense possibilities for analytical or computer prediction of dynamic tire response, and it is intended to exploit this as fully as funds and ability permit.



## II. SUMMARY

The equations describing the deformation of a circular cylindrical shell are presented in dimensionless form. The linearized version of these is solved for the case of the contact of such a shell with a flat plane representing a roadway. The length of the contact patch obtained from such a calculation is shown to approximate closely the actual patch lengths measured on an automotive tire. Similar calculations, using parameters typical of aircraft tire practice, result in patch lengths which deviate somewhat from those measured on an aircraft tire. The reasons for this deviation are given. Stresses in the running band are calculated due to both bending and inflation, and the critical pressure necessary to maintain a state of tension is given.

The primary purpose of this report is to present the equations of motion, which are believed to have wide applicability outside of the restricted problem done here, and to show that the solutions obtained from such equations seem to agree with measurements on real tires.

### III. EQUATIONS OF EQUILIBRIUM

Consider a circular shell of width  $b$  in a state of plane stress, or two-dimensional loading, so that it appears as shown in Fig. 1. The external pres-

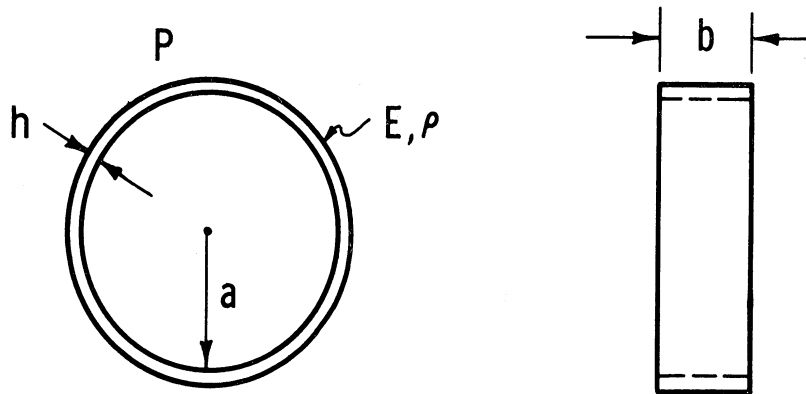


Fig. 1. Circular shell in a state of plane stress, or two-dimensional loading.

sure is denoted by  $p$ , and is positive when exceeding the internal pressure.

Considering now that the geometric midline defines the position of the thin shell, let the deformed and undeformed states be shown as in Fig. 2.

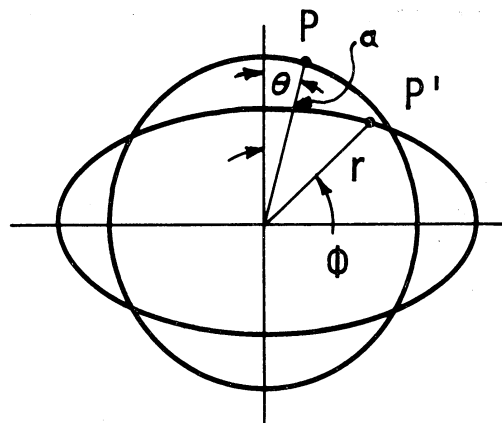


Fig. 2. Deformed and undeformed states of thin, circular shell.

Here, P represents the original position and P' the final position,  $\omega$  and  $\theta$  original coordinates, and r and  $\phi$  final ones. Define the variables

$$w = a - r \quad (1)$$

$$\zeta = \frac{w}{a} \quad (2)$$

$$\psi = \phi - \theta \quad (3)$$

Also define

$$\alpha^2 = \frac{h^2}{12a^2} ,$$

and the dimensionless time

$$\tau = \frac{t}{a} \left[ \frac{E}{\rho} \right]^{1/2} .$$

Now, letting a dot indicate differentiation with respect to  $\tau$  and a prime with respect to  $\theta$ , one finds that the dynamic equations of motion of such a shell have been derived by Goodier and McIvor,<sup>3</sup> retaining terms up to order two. Two different methods of derivation yield slightly different sets of equations. These are given as

$$\begin{aligned} \zeta'' + \alpha^2(\zeta^{IV} + 2\zeta'' + \zeta) - (\psi' - \zeta) - \left[ \zeta''(\psi' - \zeta) - \zeta^2 \right. \\ \left. + \zeta'\psi'' - \frac{1}{2}\zeta'^2 \right] - \frac{a}{Eh} p = 0 \end{aligned} \quad (4a)$$

$$\psi'' - (\psi'' - \zeta') - (\zeta'\zeta'' - 2\zeta'\psi') + \frac{a\zeta'}{Eh} p = 0 , \quad (4b)$$

while the second form is

$$\begin{aligned} \ddot{\zeta} + \alpha^2(\zeta^{IV} + 2\zeta'' + \zeta) - (\psi' - \zeta) - \left[ \zeta''(\psi' - \zeta) + \psi'^2 \right. \\ \left. - 2\zeta\psi' + \zeta'\psi'' - \frac{1}{2}\zeta'^2 \right] - \frac{a}{Eh} p = 0 \end{aligned} \quad (5a)$$

$$\ddot{\psi} - (\psi'' - \zeta') - (\zeta'\zeta'' - 2\zeta'\psi') + \frac{a}{Eh} \zeta'p = 0 \quad (5b)$$

Note that if Eqs. (4) and (5) are individually simplified by neglecting all terms of order two, they become identical. It should also be pointed out that this same simplified, linearized form is given by Flügge,<sup>4</sup> with minor variations in notation. Due to the relatively small motions involved here, Eqs. (5a) and (5b) will be linearized by neglecting all products of displacements; this gives

$$\ddot{\zeta} + \alpha^2(\zeta^{IV} + 2\zeta'' + \zeta) - (\psi' - \zeta) - \frac{a}{Eh} p = 0 \quad (6a)$$

$$\ddot{\psi} - (\psi'' - \zeta') + \frac{a}{Eh} \zeta'p = 0 \quad (6b)$$

It will further be assumed that the tread, or "running band," is primarily subjected to bending effects in the radial direction and that the membrane strain in the circumferential direction is small and may be neglected. Using the notation adapted for circumferential strain,

$$\epsilon_{\phi} = -\zeta + \psi' \simeq 0 \quad (7a)$$

Using this, Eq. (6b) becomes

$$\ddot{\psi} - \frac{d}{d\phi} (\epsilon_{\phi}) + \frac{a}{Eh} \zeta'p = 0$$

or

$$\ddot{\psi} + \zeta' \frac{a}{Eh} p = 0 \quad . \quad (7b)$$

Generally one visualizes motion of a pneumatic tire as primarily radial. This is particularly true for all those problems where the axle is considered to be held rigid, at some fixed distance from the ground plane. Under such conditions  $\ddot{\psi}$  is very small and Eq. (7) becomes unimportant to the motion. Eq. (6a) remains and, under the assumption of vanishing circumferential strain, one obtains

$$\ddot{\zeta}'' + \alpha^2 (\zeta^{IV} + 2\zeta'' + \zeta) - \frac{a}{Eh} p = 0 \quad . \quad (8)$$

Note that solutions to Eq. (8) may be used along with Eq. (7a) to define  $\psi$ , the tangential motion. In adapting Eq. (8) to a pneumatic tire, one may imagine that the pressure  $p$  is generated from several sources and, recalling that such pressure is considered positive when directed inward, these may be:

- (a) A negative pressure caused by a positive deflection  $\zeta$ , chosen in the linearized algebraic form

$$-\zeta k(\theta) \quad ,$$

where  $k$  may be dependent on  $\theta$  and represents a local spring constant or modulus of an elastic foundation. Practically, this value will be highly dependent on the inflation pressure.

- (b) A negative pressure caused by a positive rate of dimensionless deflection, chosen in the linearized algebraic form

$$- \frac{d\zeta}{dt} c(\theta) \quad ,$$

where  $c$  may be dependent on  $\theta$  and represents a distributed damping coefficient.

- (c) A positive pressure caused by contact with some external surface such as the roadway, taken in the form

$$p(\theta)$$

- (d) A negative pressure caused by centrifugal forces, in the form

$$- \rho h a \omega^2 (1-\zeta) \quad ,$$

where  $\rho$  is the density of the running band.

Note that all of these pressures are deviations from the inflated, unloaded tire. Hence, inflation pressure is not of direct importance here except as it may influence the bending characteristics or stiffness of the "running band" and the foundation modulus  $k$ .

The complete form of Eq. (8) applicable to a pneumatic tire becomes

$$\begin{aligned} \ddot{\zeta} + \frac{c(\theta)a}{Eh} \dot{\zeta} + \frac{k(\theta)a}{Eh} \zeta + \alpha^2 [\zeta^{IV} + 2\zeta'' + \zeta] \\ + \rho h a \omega^2 (1-\zeta) \frac{a}{Eh} - p(\theta) \frac{a}{Eh} = 0 \quad . \end{aligned} \quad (9)$$

Equation (9) will be considered the fundamental form of the cylindrical shell equation as modified to represent a linearized pneumatic tire. It may be used to solve a wide variety of practical problems in tire dynamics and statics. Here it will be used for a very simple example, namely the calcula-

tion of the length of the contact patch of a typical tire in contact with a plane.

It is well known from experiment that pneumatic tires, in general, exhibit contact patch lengths shorter than those predicted from the geometric intersection of the undeformed tire and a plane. This is illustrated in Fig. 3. This

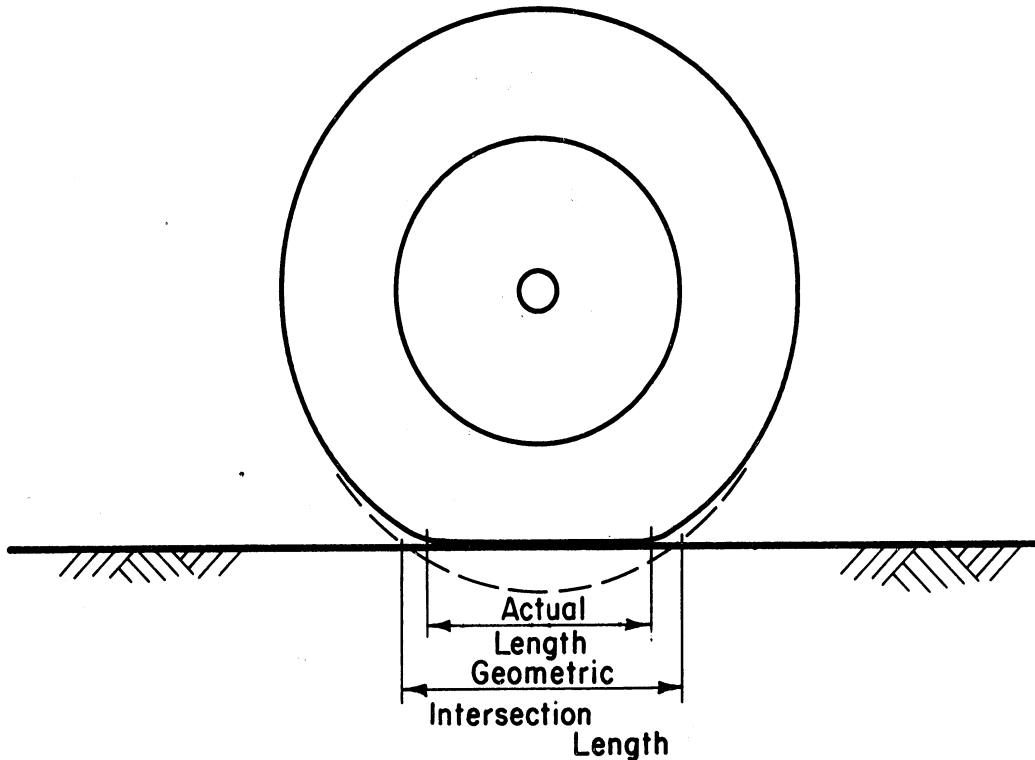


Fig. 3. Actual contact patch length vs. geometric intersection length.

effect is of particular interest in automotive tires, where the buttress-like shoulder construction causes the width of the contact patch to be fixed by the basic tread width. Here, the length of the contact area is the only dimension to change as the tire is more heavily loaded. Such pronounced shoulder constructions are not commonly used in aircraft tires, and here both the width and length can change simultaneously. The analysis which follows is clearly

more applicable to the automotive type of tire construction than the aircraft type, since the former comes much closer to the concept of the "band," represented by Eq. (9).



#### IV. CONTACT PATCH LENGTH

We next consider definition of the static-tire contact problem. Referring to Eq. (9), the term involving angular velocity  $\omega$  will of course vanish, as will terms involving time derivatives of the dimensionless radial deflection  $\zeta$ . Hence, for the static contact problem, Eq. (9) takes the special form

$$\alpha^2 \zeta^{IV} + 2\alpha^2 \zeta'' + \zeta \left[ \alpha^2 + \frac{k(\theta)a}{Eh} \right] = p(\theta) \frac{a}{Eh} \quad (10)$$

At this point it is convenient to consider the spring constant  $k$  appearing in Eqs. (9) and (10) is independent of circumferential position  $\theta$  and as a constant throughout the body of the tire. This neglects circumferential variations in the spring constant; such variations are not of particular interest in this problem since they really represent second order effects. One may further, for purposes of conciseness, introduce the symbols

$$\bar{k} = \frac{k(\theta)a}{Eh} \quad \bar{p} = \frac{p(\theta)a}{Eh} \quad (11)$$

and in these terms Eq. (10) may be written

$$\zeta^{IV} + 2\zeta'' + \left( 1 + \frac{\bar{k}}{\alpha^2} \right) \zeta = \frac{\bar{p}}{\alpha^2} \quad (12)$$

Equation (12) will represent the fundamental equation used to define contact patch length in this report.

The intersection of a circle and a plane is illustrated geometrically in Fig. 4. It shows that the geometry of intersection requires that inside the region of contact of the elastic tire with the plane the radial deflection

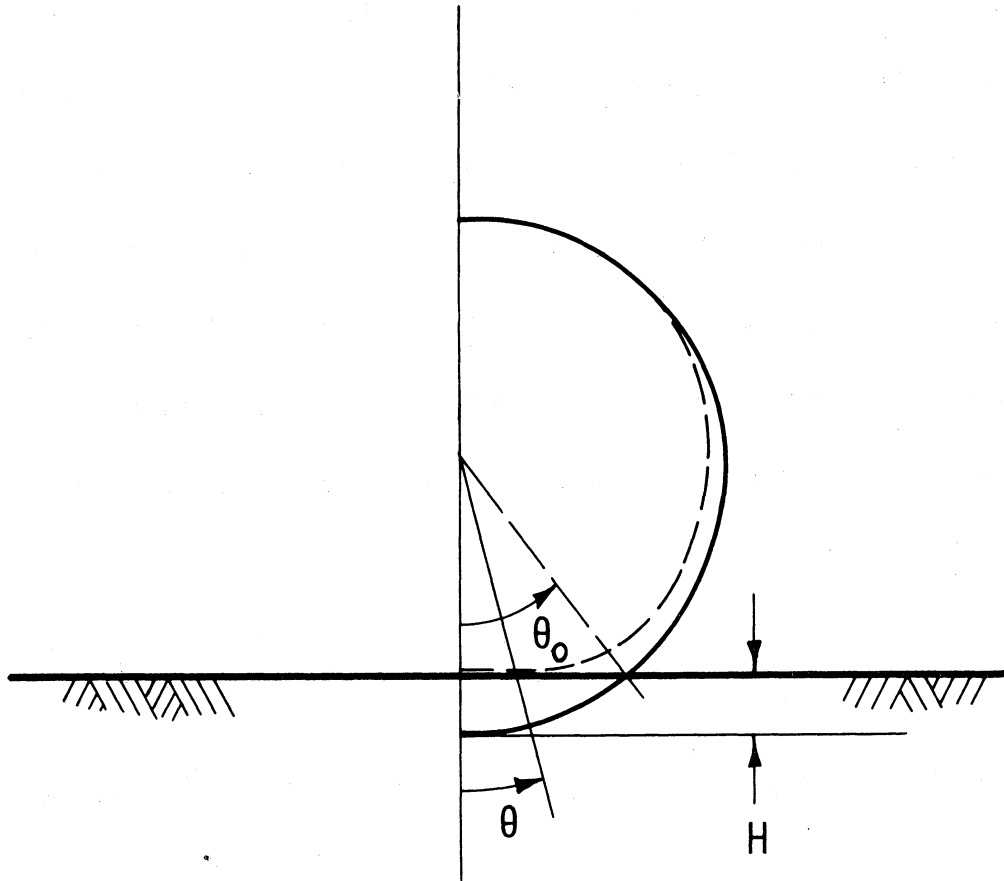


Fig. 4. Geometry of intersection of a circle and a plane.

must be

$$\zeta = \left( 1 - \frac{\cos \theta_0}{\cos \theta} \right) , \quad (13)$$

where the angle  $\theta_0$  represents the intersection of the circle of the shell and the plane.  $\theta_0$  is related to the deflection  $H$  by

$$H = a(1 - \cos \theta_0) . \quad (14)$$

Using Eq. (13), one may form the derivatives

$$\begin{aligned} \zeta'' &= - \frac{\cos \theta_0}{\cos^3 \theta} (1 + \sin^2 \theta) \\ \zeta^{IV} &= - \frac{\cos \theta_0}{\cos^5 \theta} [5 + 18 \sin^2 \theta + \sin^4 \theta] . \end{aligned} \quad (15)$$

The condition for the end of the contact patch is obtained by letting the right-hand side of Eq. (10) vanish. In doing this, one must insert the values of  $\zeta$  as given by Eqs. (13) and (15), since these are the values which will be operable in the contact patch, assuming that no buckling phenomena occur.

Carrying out this substitution, one obtains a transcendental equation for the point at which the pressure distribution  $\bar{P}$  on the shell vanishes, this point being the end of the contact patch of the real elastic tire against a plane.

This equation becomes

$$1 + \frac{\bar{k}}{\alpha^2} = \frac{\cos \theta_0}{\cos \theta} \left[ 1 + \frac{\bar{k}}{\alpha^2} + \frac{2(1+\sin^2\theta)}{\cos^2\theta} + \frac{(5+18 \sin^2\theta+\sin^4\theta)}{\cos^4\theta} \right] \quad (16)$$

where, upon examination of the definitions of  $\bar{k}$  and  $\alpha^2$ , it is seen that

$$\frac{\bar{k}}{\alpha^2} = 12 \left( \frac{k}{E} \right) \left( \frac{a}{h} \right)^3, \quad (17)$$

so that the ratio  $\bar{k}/\alpha^2$  is clearly dimensionless.

Equation (16) may be used to calculate the contact patch length of various tires, and this linearized shell theory results in a particular tire's being statically characterized by a single parameter  $\bar{k}/\alpha^2$ , this parameter being a dimensionless ratio of the linearized spring stiffness and the various bending stiffness parameters of the tire. In some ways, it might be considered a ratio of elastic bed stiffness to tread bending stiffness. As the tread bending stiffness is increased, this quantity will decrease while physical changes tending to increase the elastic spring stiffness, such as increasing the inflation pressure, will clearly increase the ratio  $\bar{k}/\alpha^2$ .

Calculation of contact patch lengths, obtained by solving Eq. (16) for

its root  $\theta$  under conditions of given  $\theta_0$ , is a somewhat tedious process if hand methods are used.  $\theta_0$  clearly defines the deflection of the tire, as pointed out in Eq. (14).

## V. COMPARISON OF CALCULATION AND EXPERIMENT

Two different methods were adopted for comparison of contact patch calculations with experiment. In the first method, a standard 8:00-14 tire manufactured by the B. F. Goodrich Tire Company was mounted in a Riehle tensile-testing machine, using a yoke arrangement so that it could be pressed against a flat steel surface with varying loads. The tread of this tire was inked, and contact patch prints were subsequently made for a variety of different deflected positions. Values of contact patch length versus deflection were obtained; some of these are shown in Fig. 5 for pressures of 15, 24, and 30 psi. These data show that there is very little apparent difference in contact patch geometry as pressure is varied over this range.

The elastic constant characterizing this particular tire was obtained from part of the test data shown on Fig. 5, in which a vertical tire deflection of 1.0 inches corresponded to a contact patch length of 8.0 inches. Upon solving for the appropriate value of  $\bar{k}/\alpha^2$ , this came out to be

$$\frac{\bar{k}}{\alpha^2} = 336 ;$$

this value was used for subsequent calculations. A simple digital computer program based on Eq. (16) was used to obtain the solutions to this transcendental equation. Using the numerical value of  $\bar{k}/\alpha^2$  just given, this program was used to calculate contact patch lengths at other values of vertical tire deflection. These are shown in Fig. 5 as the line marked "calculation."

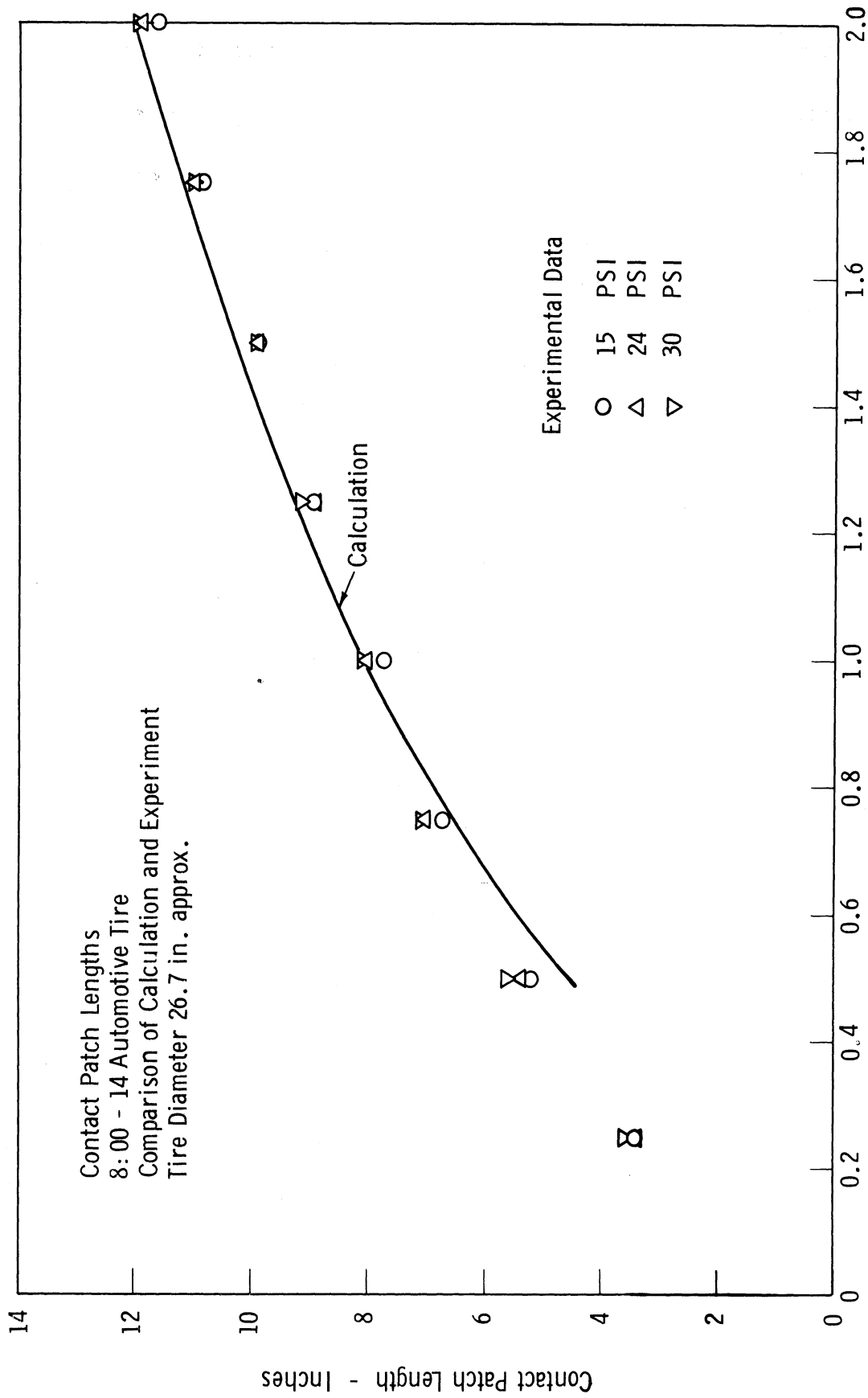


Fig. 5. Plot of contact patch length vs. vertical tire deflection.

Figure 5 shows that there is reasonably good agreement between the calculated values of contact patch length and the measured values for vertical tire deflections in excess of 0.75 inches. This agreement seems to indicate that in the region of technical interest this expression predicts contact patch length satisfactorily. For very small vertical tire deflections, the expression is not particularly successful in such predictions.

A photograph of this particular tire is given in Fig. 6.



Rather than attempt to perform experiments on an aircraft tire for purposes of comparison of the measured contact patch lengths with calculated con-

tact patch lengths, recourse was had to the considerable quantity of experimental data given in NACA Technical Note No. 4110, "Mechanical Properties of Pneumatic Tires with Special Reference to Modern Aircraft Tires" by Robert F. Smiley and Walter B. Horne. This document contains considerably more experimental data than one could reasonably hope to get economically in our laboratories. In making this comparison, it should be noted from the outset that the running band concept, and hence the idea of representing a tire by a section of cylindrical shell, is certainly less applicable to typical aircraft tire construction than to automotive tire construction. The reasons for this are the obvious geometric tread differences: in the aircraft tire the contact patch is very close to elliptical in shape and is of such a nature that upon increasing deflection the width as well as the length of the patch changes. Nevertheless, it is of some interest to examine the correlation between cylindrical shell theory and aircraft tire experiment, and for that purpose the data of Smiley and Horne was used to determine the ratio  $\bar{k}/\alpha^2$  for a typical aircraft tire. This number, based on a deflection of .06 times tire diameter, is

$$\frac{\bar{k}}{\alpha^2} = 284 \quad ,$$

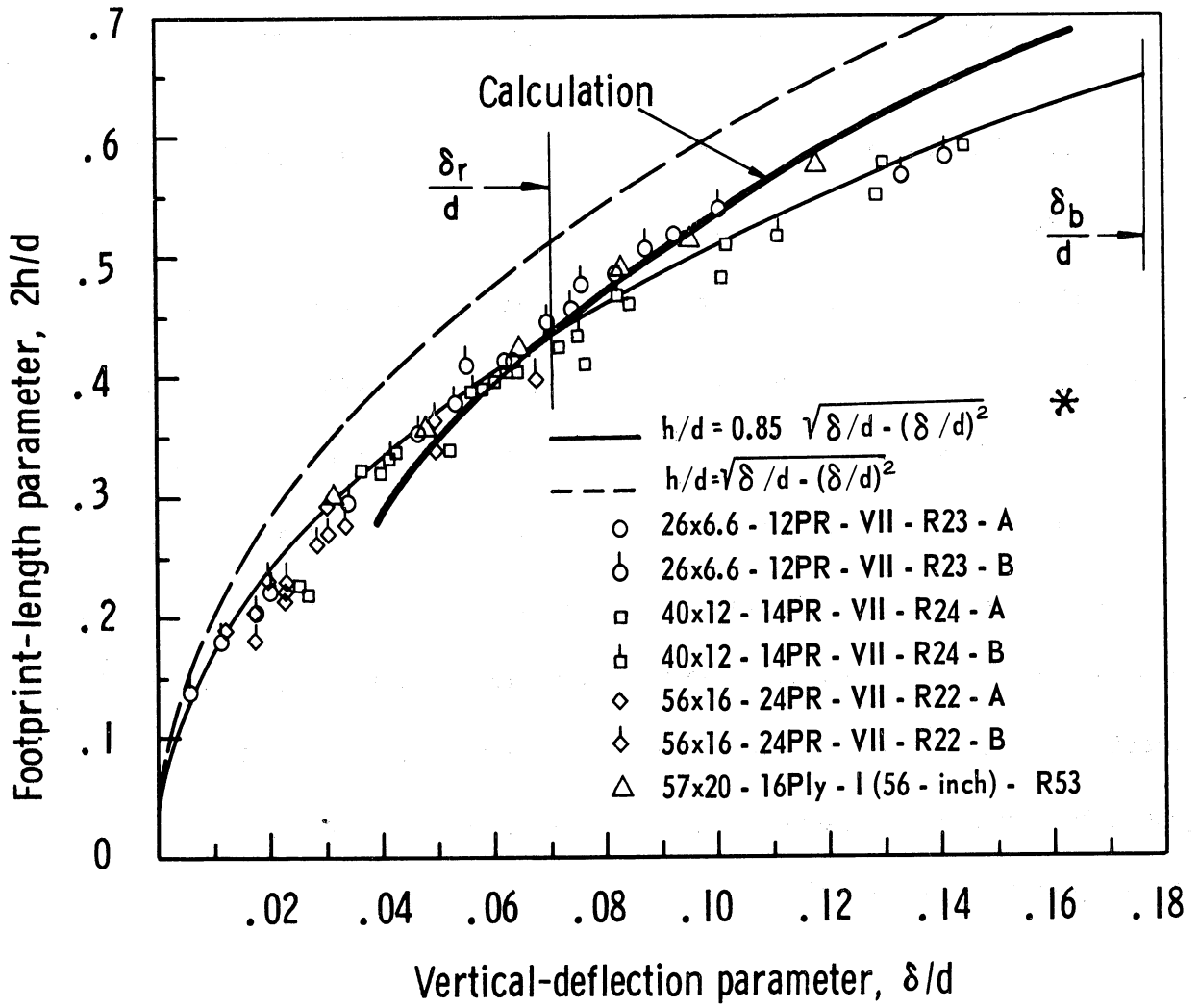
which is not too different from the value of  $\bar{k}/\alpha^2 = 336$  obtained for a typical automotive tire. This might imply that in both of these designs, apparently widely different, the ratio of elastic carcass stiffness to tread bending rigidity is very nearly the same.

Using this value of the ratio  $\bar{k}/\alpha^2$ , the same short digital computer pro-



gram representing Eq. (16) was used to determine contact patch lengths over a range of vertical tire deflections. Comparison of the calculations with the experimental data of Smiley and Horne is given in Fig. 7. It shows that the agreement is not as good as in the case of an aircraft tire, which is not particularly unexpected, but it still shows that the cylindrical shell analog predicts contact patch lengths considerably shorter than the geometric intersection lengths.

It is felt that the ability of such a simplified theory to predict accurately tire contact patch lengths represents some confirmation of the validity of this model for general tire studies. In particular, one should note that it is quite a simple matter to calculate the contact patch characteristics and pressure distribution characteristics when passing over surfaces other than the flat plane treated here. In particular, the tire running on a large test wheel, as is common in laboratory tests of various kinds, has a different contact patch length, which might readily be calculated by the techniques described here. It should also be possible by the use of these equations to handle more complicated contact situations, and it is anticipated that some of these will be covered in subsequent reports by this group.



\* Taken from Ref. 5

Fig. 7. Plot of footprint-length parameter vs. vertical-deflection parameter. From Smiley and Horne.<sup>5</sup>

## VI. STRESSES IN THE RUNNING BAND, OR TREAD, REGION

It is of considerable interest to examine the stresses in the so-called "running band," or shell, due to the imposition of both internal pressure and bending. In particular, by the use of the model described here, it should be possible to examine the value of pressure necessary to maintain tension throughout all of the running band. This would indicate, to a first approximation, the conditions necessary to keep cords in tension in this area.

This problem may be examined from the stress standpoint. Only approximate calculations will be made due to the nature of the model being used. Considering the effect of inflation first, if one assumes relatively small overall growth the internal pressure causes a circumferential stress to be uniformly distributed through the thickness of the running band whose value is

$$\sigma_1 = \frac{p_i a}{h} \quad (18)$$

where  $p_i$  = internal pressure.

A bending moment is generated in the running band due to deformation in the contact patch. This moment is given by (see Ref. 4)

$$M = \frac{Eh^3}{12a} (\zeta + \zeta'') \quad (19)$$

and is related to the maximum bending stress, at the outer fiber of the running band, by the relation

$$M = \frac{\sigma_{2\max} h^2}{6} \quad (20)$$

Hence,

$$\sigma_{2\max} = \frac{Eh}{2a} (\zeta + \zeta'') \quad (21)$$

Inside the contact patch the function  $\zeta$  may be viewed in two different ways:

- a. If the tire is assumed to have no tread, as is done in the remainder of this report, then  $\zeta$  is given by Eq. (13).
- b. If the tire is assumed to have an elastic, compressible tread then the bending moments generated should be less than those generated with no tread, from a consideration of curvature changes. Furthermore it is desired to maintain the running band in tension independent of the wear on the tread. Hence it would be conservative to neglect the presence of the tread in subsequent calculations.

By neglecting tread effects one obtains  $\zeta$  from Eq. (13), which gives

$$\sigma_{2\max} = \frac{Eh}{2a} \left[ 1 - \frac{\cos \theta_0}{\cos \theta} - \frac{\cos \theta_0}{\cos \theta} \left( \frac{1 + \sin^2 \theta}{\cos^2 \theta} \right) \right] \quad (22)$$

The sum of the positive inflation stress and the maximum negative bending stress must be greater than zero, if all cords are to remain in tension and if one further accepts the rather conservative assumption that a cord lies at the extreme outer fiber of the running band, which is certainly not the case. In fact, one may determine the minimum inflation pressure necessary to just maintain tension in the running band by equating the sum of the two stresses to zero, giving

$$\frac{Eh}{2a} \left[ 1 - \frac{\cos \theta_0}{\cos \theta} - \frac{\cos \theta_0}{\cos \theta} \left( \frac{1 + \sin^2 \theta}{\cos^2 \theta} \right) \right] + \frac{P_i a}{h} = 0 \quad (23)$$

which may also be written as

$$\left( \frac{p_i a^2}{Eh^2} \right) = \frac{1}{2} \left[ \frac{2 \cos \theta_0}{\cos^3 \theta} - 1 \right] . \quad \theta \leq \theta_0 \quad (24)$$

This latter equation represents the condition for vanishing tension under the conservative assumptions just discussed. The dimensionless product

$$\frac{p_i a^2}{Eh^2}$$

is seen to be a function of the dimensionless tire deflection  $\theta_0$ . The maximum value of the right hand side of this equation occurs when the angle  $\theta$  equals  $\theta_0$ . Hence, the most critical spot for tread compression is the beginning and ending of the contact patch, so that maximum pressures are given by

$$\frac{p_i a^2}{Eh^2} = \frac{1}{2} \left[ \frac{2}{\cos^2 \theta_0} - 1 \right] . \quad (25)$$

These may be plotted conveniently in Fig. 8, from where it is seen that the critical value of this dimensionless pressure function ranges between 0.5 and 1.2 for most values of deflection.

From these expressions it is seen that tension can be maintained in the running band by keeping inflation pressure high, or running band thickness low. To take some simple examples, let

$$\frac{p_i a^2}{Eh^2} = 1$$

and further let

$$a = 10 \quad h^2 = 10^{-1} \quad E = 10^5$$

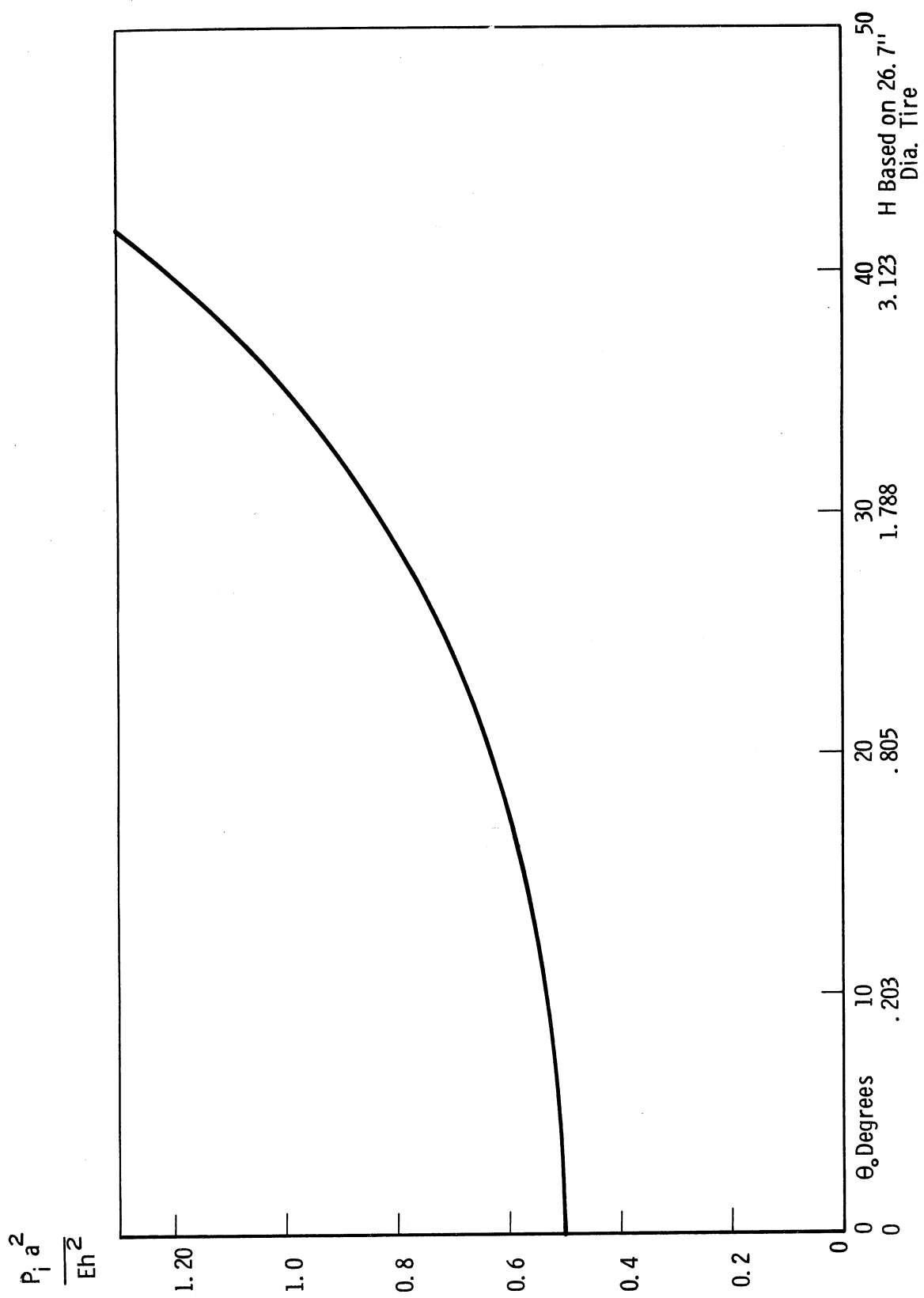


Fig. 8. Critical pressure necessary to maintain tension in the running band.

then

$$p_i = 100 \text{ psi} .$$

On the other hand, let

$$h^2 = 10^{-2}$$

and

$$p_i = 10 \text{ psi} .$$

In view of the rather conservative assumptions made in arriving at this pressure, which will certainly be lower than the values given above, it appears that it might be within the realm of possibility to construct a tire such that the running band was always in tension.

## VII. REFERENCES

1. Saito, Y., "A Study of the Dynamic Steering Properties of Pneumatic Tires," 9th International Automobile Technical Congress, 1962, published by the Institution of Mechanical Engineers, London.
2. Thorsen, K. R., 1951 Boeing Airplane Company Report No. D-11719, "A Rational Method for Predicting Tire Cornering Forces and Lateral Stiffness."
3. Goodier, J. N. and McIvor, I. K., "The Elastic Cylindrical Shell Under Nearly Uniform Radial Impulse," ASME Paper No. 63-APMW-6, 1963.
4. Flügge, Wilhelm, "Stresses in Shells," Springer-Verlag, Berlin, 1960.
5. Smiley, Robert F. and Horne, Walter B., "Mechanical Properties of Pneumatic Tires with a Special Reference to Modern Aircraft Tires," National Advisory Committee for Aeronautics, Technical Note No. 4110, Langley Aeronautical Laboratory, Langley Field, Virginia, January 1958.



VIII. DISTRIBUTION LIST

	No. of Copies
The General Tire and Rubber Company Akron, Ohio	6
The Firestone Tire and Rubber Company Akron, Ohio	6
B. F. Goodrich Tire Company Akron, Ohio	6
Goodyear Tire and Rubber Company Akron, Ohio	6
United States Rubber Company Detroit, Michigan	6
S. S. Attwood	1
R. A. Dodge	1
The University of Michigan ORA File	1
S. K. Clark	1
Project File	10



3 9015 02828 5370